

Catalysis Science & Technology

Accepted Manuscript



This article can be cited before page numbers have been issued, to do this please use: Y. Jiao, M. S. Torne, J. Gracia, J. W. Niemantsverdriet and P. W.N.M. van Leeuwen, *Catal. Sci. Technol.*, 2017, DOI: 10.1039/C6CY01990K.



This is an Accepted Manuscript, which has been through the Royal Society of Chemistry peer review process and has been accepted for publication.

Accepted Manuscripts are published online shortly after acceptance, before technical editing, formatting and proof reading. Using this free service, authors can make their results available to the community, in citable form, before we publish the edited article. We will replace this Accepted Manuscript with the edited and formatted Advance Article as soon as it is available.

You can find more information about Accepted Manuscripts in the [author guidelines](#).

Please note that technical editing may introduce minor changes to the text and/or graphics, which may alter content. The journal's standard [Terms & Conditions](#) and the ethical guidelines, outlined in our [author and reviewer resource centre](#), still apply. In no event shall the Royal Society of Chemistry be held responsible for any errors or omissions in this Accepted Manuscript or any consequences arising from the use of any information it contains.

Ligand Effects in Rhodium-Catalyzed Hydroformylation with Bisphosphines: Steric or Electronic?

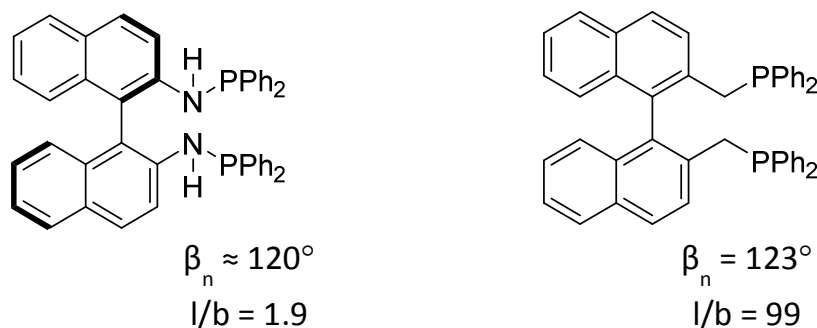
Yunzhe Jiao^{*†‡}, Marta Serrano Torne[‡], Jose Gracia[†], J. W. (Hans) Niemantsverdriet^{†#}
and Piet W. N. M. van Leeuwen^{*‡&}

[‡]*Institute of Chemical Research of Catalonia (ICIQ), The Barcelona Institute of Science and Technology, Avda. Paisos Catalans 16, 43007 Tarragona, Spain*

[†]*SynCat@Beijing, Synfuels China Technology Co. Ltd, Beijing, P. R. China*

[#]*Syngaschem BV, PO Box 6336, 5600 HH Eindhoven, The Netherlands*

[&]*Present address: LPCNO, INSA-Toulouse, 135 Avenue de Rangueil, F-31077 Toulouse, France*



Do wide bite angles lead to high linear regioselectivity in hydroformylation, or is an electronic effect operative?

Abstract

Twelve commercially available bisphosphine ligands have been evaluated in rhodium-catalyzed hydroformylation reactions. All ligands exhibited high chemoselectivities for aldehyde formation. The highest enantioselectivity (53% ee) of

styrene hydroformylation was achieved with (S)-BTFM-Garphos (**L7**) substituted with electron withdrawing substituents. High pressure NMR (HP-NMR) and *in situ* high pressure IR spectroscopy (HP-IR) were used to study the resting states of the catalyst species in the reactions. The ligand effect on the structures of the observable species was examined. Both electronic and steric factors were considered to contribute to the performance of the various ligands. The results showed that decreasing the phosphine basicity increased the enantioselectivity, while in the systems studied here the steric character plays a less important role than the electronic feature in achieving good regioselectivities.

Introduction

Hydroformylation is one of the most extensively studied homogeneous catalytic processes in industry.¹⁻³ Much effort has been devoted to the development of catalysts/ligands in order to obtain high catalytic activities and selectivities. Compared to the diphosphite ligands with good enantioselectivities in limited examples, bisphosphine ligands such as bisdiazaphospholanes and bisphospholanes have been reported to achieve excellent ee values and enhanced efficiency in asymmetric hydroformylation with a wide range of substrates.^{4,5} For instance, the use of the diazaphospholane ligands gives ee values of 86-99% in the asymmetric hydroformylation of *N*-vinyl carboxamides, allyl ethers, and allyl carbamates.⁶ Nevertheless, there is a need for novel bisphosphine ligands, especially chiral ones, to broaden the substrate scope in hydroformylation.

In order to be able to predict the performance of a candidate ligand, it is necessary to establish the relationship between ligand structure and the catalytic species formed in the reaction. In general, bidentate phosphorus ligands form a pentacoordinate

intermediates $\text{HRh}(\text{P-P})(\text{CO})_2$ (P-P = bisphosphine), which play a decisive role in determining the regioselectivity and enantioselectivity of the reaction.^{7,8} In this study, *in situ* spectroscopic experiments were conducted under the ‘real’ catalytic conditions to monitor the reaction and the catalyst’s resting states. The formation of a single catalytic species was suggested to be the key to maintain high enantioselectivities while other species can also be present, as shown in high-pressure infrared (HPIR) absorption.^{9–11} The trigonal bipyramidal hydridorhodium complex equilibrates between two possible isomeric structures of different phosphine-coordination modes: equatorial-apical (**ea**) or equatorial-equatorial (**ee**) coordination, as derived from the coupling constants in high-pressure NMR (HPNMR).¹² Although the **ee** coordination mode is generally related to a wide bite angle and high linear/branched ratios, the regioselectivities of the reaction were not predictable solely from the chelation mode of the bisphosphine in $\text{HRh}(\text{P-P})(\text{CO})_2$.¹³

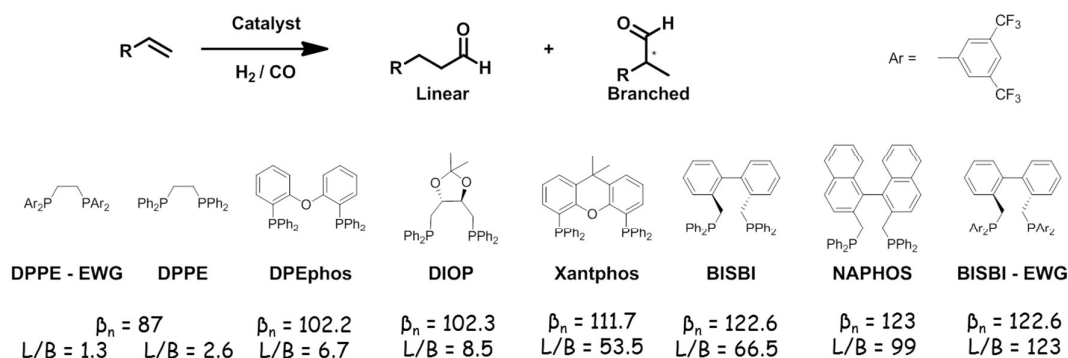


Fig. 1 Bite angle effect in l/b ratio using different bisphosphine ligands in the Rh-catalyzed hydroformylation of 1-alkenes.^{12–19}

As shown in Fig. 1, the steric effect is demonstrated in the reaction as increasing the bite angle of the ligand usually leads to a higher regioselectivity in the hydroformylation.^{12,20} For example, the linear/branched (l/b) ratio increased from 2.6

with DPPE ($\beta_n = 87^\circ$) to 99 with NAPHOS ($\beta_n = 123^\circ$).^{19–23} An even higher linearity preference ($l/b = 123$) was observed for the BISBI derivative with CF_3 substitution on the aryl rings at phosphorus.²⁴ However, a negative effect of electron withdrawing substituents on regioselectivities was observed in bisphosphines such as the DPPE ligands, which have small bite angles, with the resulting coordination at **ea** sites (the numbers were not corrected for the formation of 2-alkene side products).

In this work, we examined a series of commercially available bisphosphine ligands in the rhodium-catalyzed hydroformylation of 1-octene and styrene. None of these have been previously applied in alkene hydroformylations. Our experimental results indicated that both steric and electronic character can affect the catalyst performance, although unfortunately generalization of these effects cannot be made due to limited data. Moreover, *in situ* techniques allowed us to determine the structures of the dominant species, where the chelation modes of $\text{HRh}(\text{P-P})(\text{CO})_2$ are largely influenced by the steric factor of ligands.

Materials and methods

Materials

All reactions were carried out using standard Schlenk techniques under nitrogen or argon atmosphere. Toluene was collected from the solvent purification system (MBraun MB SPS800). Toluene- d_8 was dried, distilled over sodium/benzophenone for the HP-NMR experiment. Other solvents were purged with argon before use.

2-MeTHF (anhydrous) was purchased from Sigma-Aldrich and used without further drying. Cyclohexane were purchased from Scharlab and used without further drying. DPEphos was purchased from Sigma-Aldrich. All the other bisphosphine ligands were purchased from Strem Chemicals. 2-MeTHF, styrene and 1-octene were filtered over neutral

alumina before use to remove hydroperoxides. ^1H and $^{31}\text{P}\{^1\text{H}\}$, ^{31}P NMR spectra were recorded on a Bruker 400 or 500 MHz spectrometer. Gas Chromatography was performed on an Agilent 6890N, HP5 column. Enantiomeric excesses were measured on the same equipment with β -dex 120 column. Standard infrared spectra were recorded on a Thermo Nicolet FT-IR 5700 Nexus spectrometer equipped with a MCT detector, KBr beam splitter at 4 cm^{-1} resolution. High-pressure transmission IR experiments were performed in a 50 mL autoclave (SS 316) equipped with IRTRAN windows (ZnS), a mechanical stirrer, a temperature controller, and a pressure transducer; home-built by the workshop of the FNWI, University of Amsterdam.²⁵

Standard hydroformylation experiments

A solution of $\text{Rh}(\text{acac})(\text{CO})_2$ (0.005 mmol) and the phosphorus compound (0.01 mmol) were dissolved in 4 mL toluene and injected into the autoclave under N_2 . The syngas was introduced and the heating and stirring was initiated for catalyst incubation. Then 1 mL solution of substrate (5 mmol) was injected under syngas, followed by reaching the reaction conditions. Reaction solutions were quenched immediately with excess tri-*n*-butyl phosphite to avoid isomerization after the reaction. Conversions and regioselectivities were determined by GC analysis of the crude samples after filtration through silica gel.

In situ HP-IR experiments

The rhodium complex $\text{Rh}(\text{acac})(\text{CO})_2$ (0.052 mmol) and the corresponding phosphorus ligand (2 to 10 equiv.) were dissolved in 20 mL of 2-MeTHF. This solvent was used due to the lack of absorptions in the range of CO stretching bands and the solvent effect is small considering the polarity change between toluene and 2-MeTHF.^{26,27} After the

HP-IR autoclave had been pressurized and the mixture heated, the autoclave was placed in the infrared spectrometer. While the sample was being stirred the infrared spectra were recorded.

HP-NMR experiments

The rhodium complex Rh(acac)(CO)₂ (0.04 mmol) and the corresponding phosphorus ligand (0.08 mmol) were dissolved in toluene-d₈ (0.4 mL), incubated for 1 hour under 10 bar of syngas at 80 °C. A portion of the resulting solution (0.2 mL) was transferred to a sapphire tube (diameter = 10 mm) and pressurized with 10 bar of syngas. The tube was placed in a Bruker 500 MHz spectrometer and the spectra were recorded at variable temperatures.

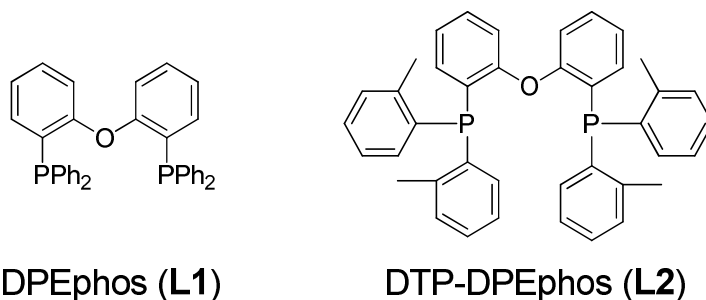
Computational details

DFT calculations with the B3LYP²⁸ and M062²⁹ functionals have been carried out with the gaussian09 program package³⁰. In M062 calculations, the combination of a 6-31G** basis set for light atoms (C, H, O, N, and F) and SDDALL for heavy atoms (P and Rh) was used for initial structure optimization. Final optimization was conducted using LANL2DZ for all atoms in both M062 and B3LYP calculations. Frequency calculations have been carried out at the optimized structures to confirm that they are minima on the potential energy surface. Because of the polarity of the structures, the solvent effects on their relative stabilities were evaluated by calculating the free energies of the solvation in terms of the polarizable continuum model (PCM). Gibbs free energies have been calculated at 298.15 K and 1 atm.

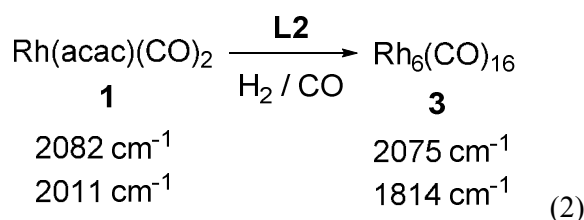
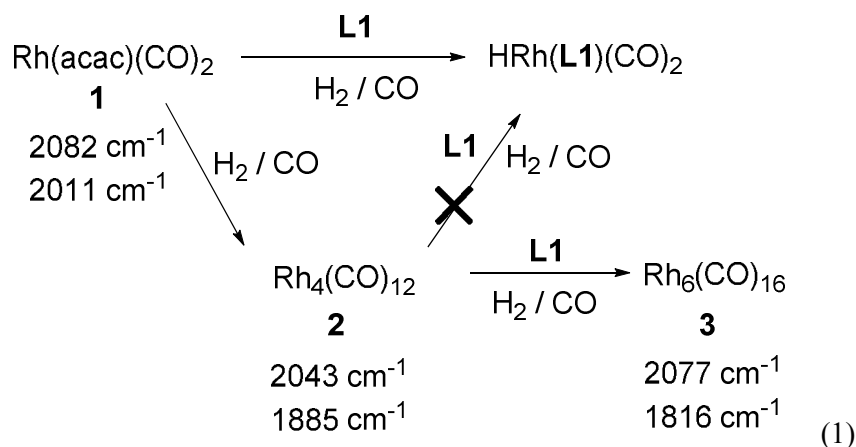
Results and discussions

***In Situ* HP-IR Analysis of Rhodium-DPEphos/DTP-DPEphos**

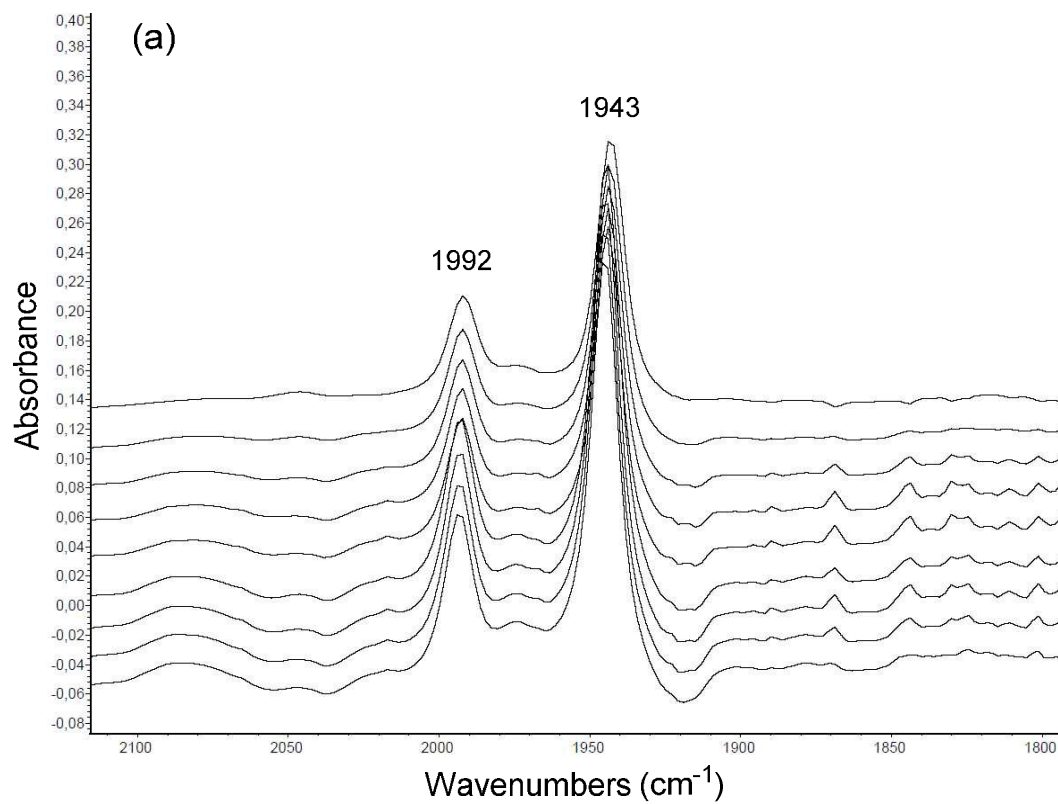
As shown in Scheme 1, DPEphos (**L1**) has proved to be a good ligand for hydroformylation with a high selectivity and a moderate activity. Its *o*-tolyl derivative DTP-DPEphos (**L2**) has a few applications in Heck coupling and aryl halide amination but has not been tested in hydroformylation.^{31,32} While steric factors are held responsible for the determination of the *l/b* ratio in hydroformylation³³, these steric effects are brought about by changing the backbone and there are hardly examples of steric variations of the substituents on phosphorus using the same backbone. To compare the substituent effect, *in situ* HP-IR and HP-NMR techniques were used to determine the dominant species present during the reaction of the typical rhodium precursor Rh(acac)(CO)₂ (**1**) and the ligand. HP-FTIR was performed under 20 bar of syngas at RT to 80 °C. In the reaction of **L1**, precursor **1** was depleted too fast to be observable from comparison with the reported IR absorptions (2082, 2011 cm⁻¹). Instead, two peaks at 1992 and 1943 cm⁻¹ appeared immediately after pressurization at r.t. (Fig. 2(a)). The frequencies can be assigned as HRh(CO)₂(**L1**) by comparison with the reported absorptions for the type of hydride species HRh(CO)₂(P-P) with **ea** phosphorous coordination (Table 1).^{12,34}



Scheme 1 Nonchiral bisphosphine ligands **L1** and **L2** for hydroformylation.



During heating to 80 °C, HRh(CO)₂(L1) remained as the only formed species within terminal carbonyl region and did not change after substrate addition, suggesting HRh(CO)₂(L1) as the resting state in the catalytic cycle. The same species were observed in using cyclohexane instead of 2-MeTHF as the solvent, indicating the independence on the solvent polarity. As shown in Fig. 2(b), a new band appeared at 1885 and 2043 cm⁻¹ with the decay of **1** under pressurization of syngas in the absence of any phosphine ligand. This species is attributed to Rh₄(CO)₁₂ (**2**) (reported ν/cm⁻¹: 1885.4, 2044.2, 2071.2)³⁵ with the assumption that the other major bands are covered by the peak at 2077 cm⁻¹ from the subsequent rapid formation of Rh₆(CO)₁₆ (**3**) (observed ν/cm⁻¹: 1816, 2077; reported ν/cm⁻¹: 1818.4, 2075.4)³⁵ (Fig. 2(b), eq 1). The formation of **2** is irreversible as the following injection of ligand did not give the expected formation of HRh(CO)₂(L1).



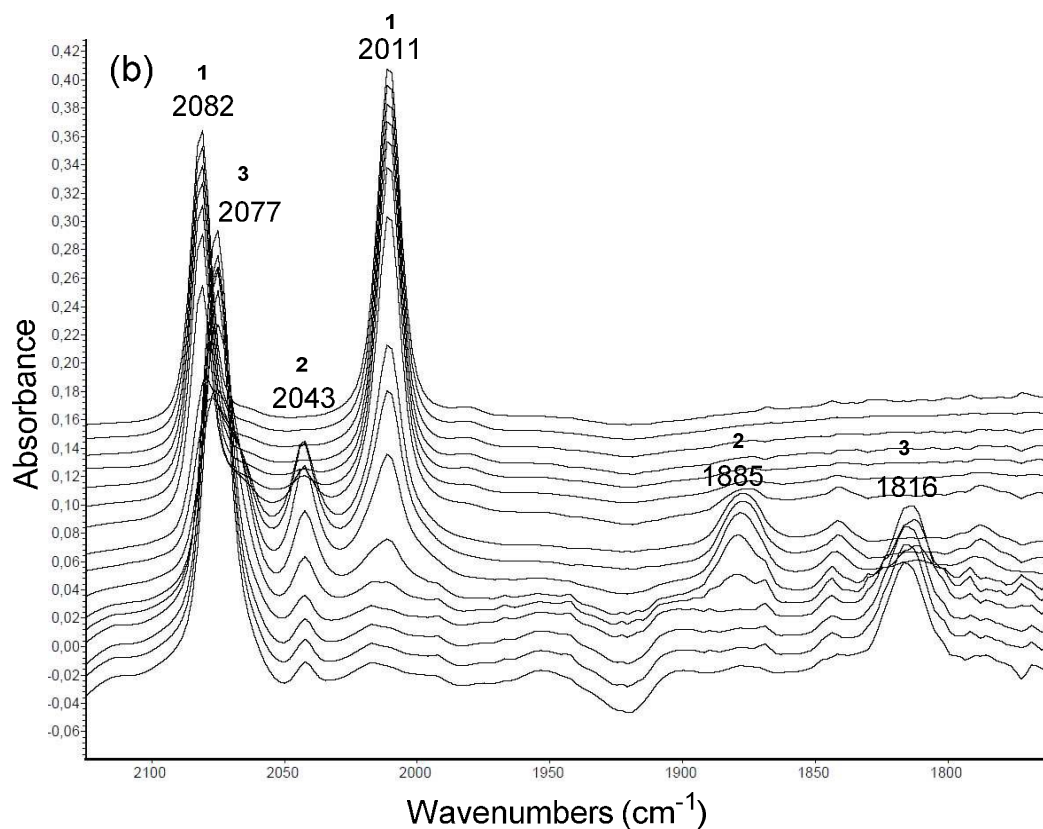


Fig. 2 (a) HP-FTIR spectra for the reaction of **1** with **L1** in 2-MeTHF at 80 °C, 20 bar of CO/H₂ (1:1) (carbonyl region). (b) HP-FTIR spectra for the reaction of **1** without any phosphine ligand in 2-MeTHF at 80 °C, 20 bar of CO/H₂ (1:1) (carbonyl region). Spectra were recorded from top to bottom.

In contrast, no occurrence of HRh(CO)₂(**L2**) was observed during an HP-IR experiment of **L2** under the same condition (Fig. 3, eq 2). The metal precursor **1** disappeared within one hour during heating and correspondingly **3** formed as the first intermediate. The minor peak at 2042 cm⁻¹ might be from the formation of **2**. Within four hours at 80 °C, decomposition of **3** occurred, leaving one major peak at 2038 cm⁻¹.

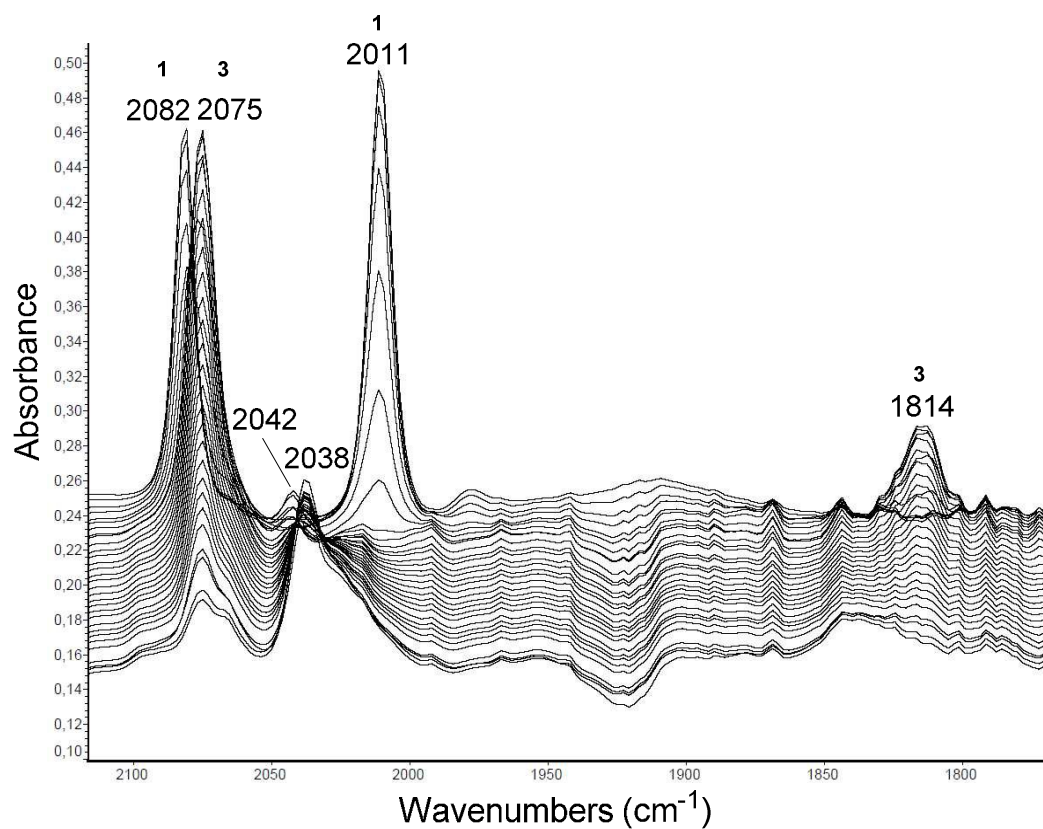


Fig. 3 HP-FTIR spectra for the reaction of **1** with **L2** in 2-MeTHF at 80 °C, 20 bar of CO/H₂ (1:1) (carbonyl region). Spectra were recorded from top to bottom.

Table 1 HP-FTIR data of the species formed in the hydroformylation reaction.

Complexes	IR ν_{ee} (cm ⁻¹)	IR ν_{ea} (cm ⁻¹)
HRh(CO) ₂ (L1)	--	1992, 1943
HRh(CO) ₂ (L4)	2044, 1967	--
HRh(CO) ₂ (L6)	--	1990, 1948
HRh(CO) ₂ (L7)	--	2010, 1970
HRh(CO) ₂ (CHIRAPHOS) ^a	--	2000, 1961
HRh(CO) ₂ (BDPP) ^a	--	1988, 1944
HRh(CO) ₂ (SPANPhos) ^a	2027, 1978	2039, 2005, 1949

HRh(CO) ₂ (pySPAN) ^a	2063, 2009	--
HRh(CO) ₂ (PPh ₃) ₂ ^a	2042, 1981	1992, 1947
HRh(CO) ₂ (PEtPh ₂) ₂ ^a	2037, 1979	1990, 1947

^a Reported absorptions for the type of hydride species HRh(CO)₂(bisphosphine).^{12,33}

High Pressure NMR Analysis of Rhodium-DPEphos Pretreatment

To confirm the structures of the resting states formed from precursor and ligand, HP-NMR spectra were measured after the reaction between **1** and **L1**. Concentrated rhodium solution was prepared in order to achieve good signal to noise ratio. The ¹H NMR signals (Fig. 4) support the formation of HRh(CO)₂(**L1**), with a typical triplet of doublets for the hydride at δ -8.78 (¹J_{Rh-H} = 10.8 Hz, ²J_{P-H} = 44.7 Hz) due to the coupling of the hydride with two (time-averaged) equivalent phosphorus atoms and the rhodium atom. The coupling constants smaller than those reported for HRh(CO)₂(BDPP) (δ -8.8, ¹J_{Rh-H} = 11 Hz, ²J_{P-H} = 57 Hz)¹⁴ correspond to the decreased phosphine basicity of **L1**. The minor signal at δ -9.23 (quartet, J_{Rh-H} = 12,6 Hz) is assigned to HRh(**L1**)₂(CO) based on the reported BDPP analog HRh(BDPP)₂(CO) (δ -10.2, ¹J_{Rh-H} = 16 Hz)³⁶, in which one of the two bisphosphines coordinates to rhodium in a monodentate fashion (Table 2).

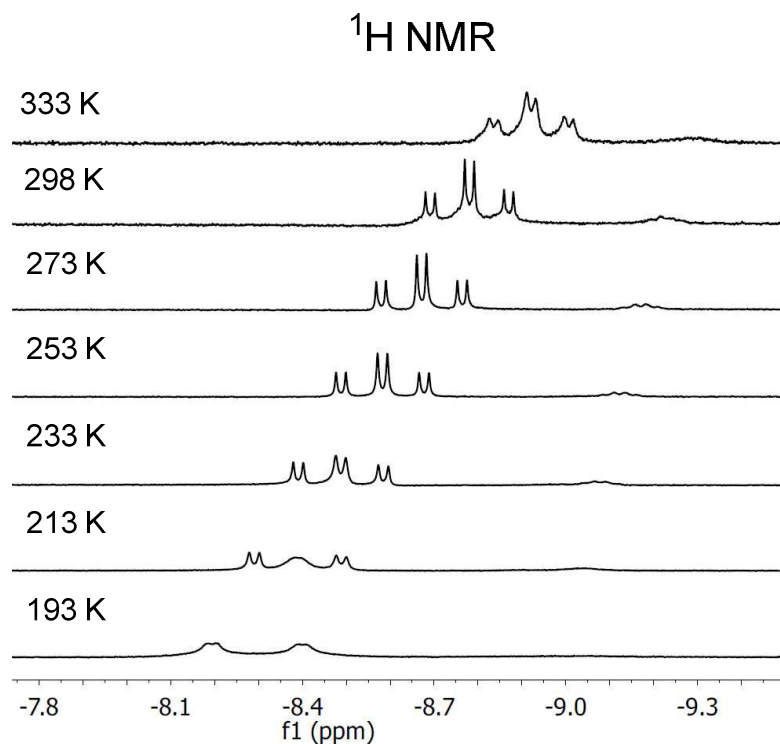


Fig. 4 ^1H NMR spectra for the reaction of **1** with **L1** in toluene- d_8 at 80 °C, 10 bar of CO/H_2 (1:1) after 1 h.

The corresponding $^{31}\text{P}\{^1\text{H}\}$ NMR spectrum showed a mixture of two doublets as well as the singlets belonging to the free phosphines and phosphine oxide. The doublet at δ 28.03 ppm was attributed to $\text{HRh}(\text{CO})_2(\text{L1})$, which has an averaged Rh–P coupling constant of 117.4 Hz (Table 2; see SI, Fig. S-1). When the temperature was decreased to -80 °C, the doublet broadened and resolved into two separate broad doublets at δ 32.4 and 25.5 ppm. All evidence suggests an **ea** geometry for $\text{HRh}(\text{CO})_2(\text{L1})$, in which the equatorial phosphorus atom has a small Rh– P_{cis} coupling constant and the apical phosphorus has a typical larger Rh– P_{trans} coupling constant. Due to the electronic difference, the Rh– P_{trans} coupling constant in $\text{HRh}(\text{CO})_2(\text{L1})$ ($^1J_{\text{Rh-P}} = 117.4$ Hz) is slightly smaller than that in **ea**- $\text{HRh}(\text{BDPP})_2(\text{CO})$ ($^1J_{\text{Rh-P}} = 120.0$ Hz). ^{31}P NMR showed a double doublet at RT, in which the size of $^2J_{\text{H-P}}$ of 43.2 Hz again indicated the fast

exchange of the two phosphorus atoms in equatorial and apical positions at room temperature (see SI, Fig. S-2). However, in this instance the distinct axial P–H and equatorial P–H coupling was not observable even at $-80\text{ }^{\circ}\text{C}$.

The other broad doublet at δ 11.56 ($J_{\text{Rh-P}} = 153.8\text{ Hz}$) was tentatively assigned to a dimer species $[(\mathbf{L1})\text{Rh}(\text{CO})_2]_2$ (see SI, Fig. S-2). However, instead of the expected two pairs of doublets for restricted rotation at low T as reported previously for $[\text{Rh}(\text{BDPP})(\text{CO})_2]_2$ ³⁶, four sets of doublets appeared at δ 20.9, 12.7, 10.2, 3.5 with respective coupling constants of 187, 113, 113, 187 Hz at $-80\text{ }^{\circ}\text{C}$ for the unknown structure. Skewed structures of **L1** could lead to a lower symmetry, but we have no proof for that.

Table 2 ^1H and $^{31}\text{P}\{^1\text{H}\}$ NMR data of the species formed under hydroformylation conditions ($80\text{ }^{\circ}\text{C}$ and 10 bar of 1:1 CO/H_2).

Complex	^1H NMR			$^{31}\text{P}\{^1\text{H}\}$ NMR	
	$\delta(\text{ppm})$	$^1J_{\text{Rh-H}}(\text{Hz})$	$^2J_{\text{P-H}}(\text{Hz})$	$\delta(\text{ppm})$	$^1J_{\text{Rh-P}}(\text{Hz})$
ea -HRh(CO) ₂ (L1)	-8.78	10.8	44.7	28.03	117.4
HRh(L1) ₂ (CO)	-9.23	12.6	---	---	---
ea -HRh(CO) ₂ (L7)	-9.21	9.6	62.5	44.71	120.0
ea -HRh(CO) ₂ (BDPP)	-8.8	11	57	29.8	112
HRh(BDPP) ₂ (CO)	-10.2	16	---	---	---
HRh(PEtPh ₂) ₃ (CO)	-10.1	br	---	34.5	150

Hydroformylation of 1-Octene with L1 and L2: Ligand Effect on Catalyst Performance

L1 and **L2** were examined in the hydroformylation of 1-octene under various conditions (eq 3). The reaction was carried out at 80 °C and 20 bar of 1:1 CO/H₂ using a 1.0 mM solution of rhodium precursor **1** and the corresponding bisphosphine ligand. The ligand/metal (L/M) ratio was varied at 3, 5, 10 and 15 to study the effect of ligand concentrations on the catalytic activity of hydroformylation. The product mixtures were monitored by gas chromatography and the results are summarized in Table 3. For **L1**, our results are identical to the reported value with a smaller L/M ratio.¹² The increase of ligand/metal ratio slows down the reaction a little and has minimal influence on the linear selectivity. Compared to **L1**, the tolyl derivative **L2** showed higher activities but lower selectivities for aldehyde due to alkene isomerization. Also, the linearity (l/b ratio) is less favored with **L2** than **L1**, which can be attributed to the fact that **L2** cannot coordinate to rhodium as found in the *in situ* spectroscopic studies. The failure of phosphine coordination to rhodium is due to the increased steric hindrance of **L2** and the competition of CO. The resulting high activities are not surprising because the dominant species HRh(CO)₄ (**2**) is an active catalyst in hydroformylation but usually has low selectivity control. The dissociative behavior of bulky monodentate ligands has been previously reported under hydroformylation conditions, forming unselective Rh₆(CO)₁₆ (**3**).³⁷ Addition of excess **L2** can inhibit the olefin isomerization and slightly increase the l/b ratio.

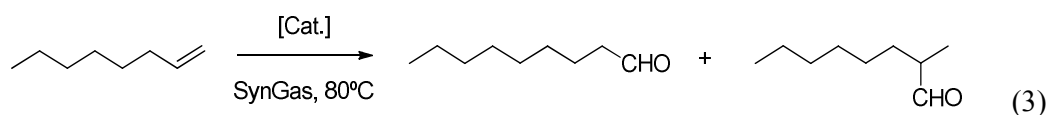


Table 3 Hydroformylation of 1-octene with the Rh(acac)(CO)₂/Ligand system. ^a

Ligand	L/M	Conv. (%)	Aldehyde Sel. (%)	Regioselectivity. (linear %)	l/b ratio
L1	3	67	100	87	6.7
L1	5	61	100	87	6.8
L1	10	57	100	87	6.8
L1	15	59	100	87	6.9
L2	3	99	42	25	1.4
L2	5	99	46	27	1.4
L2	10	99	59	36	1.6
L2	15	99	61	38	1.7
L1^b	2.2	---	100	87	6.7

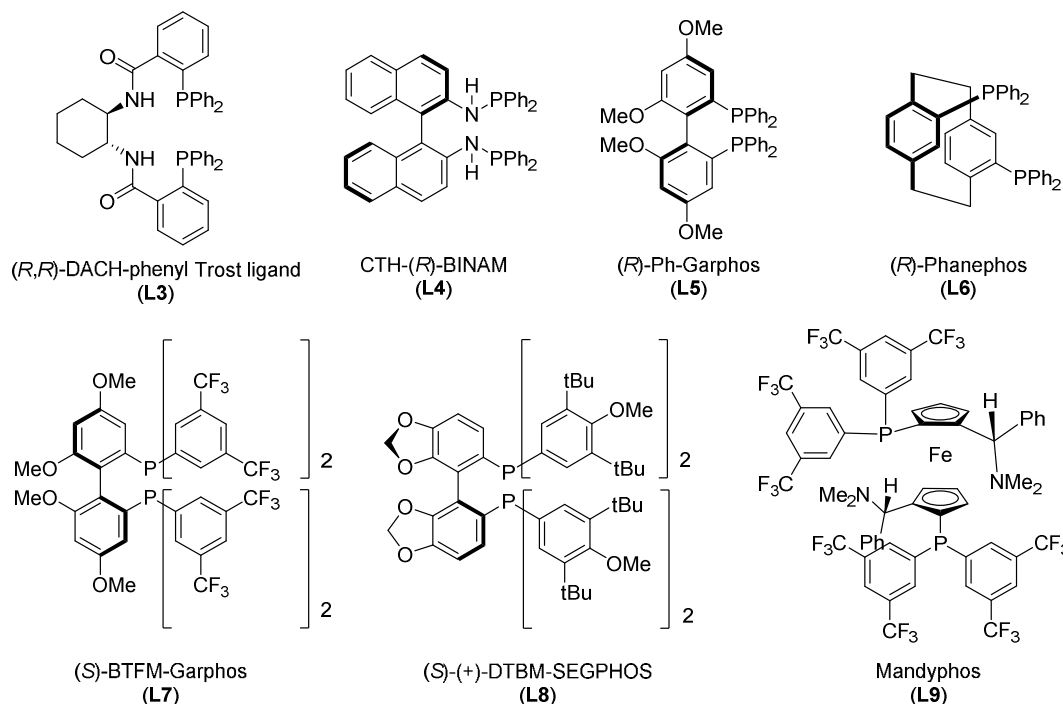
^a Reaction conditions: P(CO)/P(H₂) = 1, P(CO/H₂) = 20 bar, substrate/Rh = 667, Rh(acac)(CO)₂ = 1 mM. Incubation at 60 °C, 45 mins, 10 bar; Reaction at 80 °C, 12 h, 20 bar. ^b Previously reported reaction at P(CO)/P(H₂) = 1, P(CO/H₂) = 10 bar, substrate/Rh = 674, Rh(acac)(CO)₂ = 1.78 mM, 80 °C, 16 h.

The fast formation of the active species at r.t. in the HP-IR experiment implies that pretreatment of catalyst with **L1** is not necessary. Therefore, catalytic activities were compared under different incubation conditions (see SI, Table S-2). As expected from the spectroscopic studies, similar conversions, aldehyde selectivities, and l/b ratios were observed regardless of the incubation conditions.

Hydroformylation of 1-Octene with Chiral Ligands

Seven commercially available chiral bisphosphines **L3–9** were tested in rhodium-catalyzed hydroformylation of 1-octene (Scheme 2, Table 4). Dominating formation of internal octenes was seen when **L5** and **L8** were used. For **L8** this can be understood from the steric bulk on the aryl groups; from DFT calculations it is known that two aryl groups on two phosphine atoms during hydroformylation show π -stacking and the bulky groups prevent this. All other ligands showed high activities and selectivities to aldehydes. The formation of the linear aldehyde (1-nonanal) is slightly favored over the branched product (2-nonanal). The low l/b ratios for **L3** and **L4** are unexpected considering their wide bite angles of over 120° , although at too wide angles the relationship breaks down. In addition **L3** is highly flexible and the amides may participate in the coordination, as seen in Pd chemistry. As a high linearity is usually correlated to bidentate phosphines with large β_n (NAPHOS: $\beta_n = 123^\circ$, $l/b = 99$)¹⁹, the inclusion of the hetero N-atom in **L4** must change the selectivity by electronic means as a considerable P–N double bond character via π -interaction, indicated by the trigonal planar geometry around the nitrogen atoms, has been observed in aminophosphines.³⁸ For **L6** a behaviour similar to DPEphos might be expected in view of the bite angles, but perhaps this is counteracted by the rigidity of **L6**. On BISBI and Xantphos ligands electron withdrawing groups such as CF_3 (as present in **L7** and **L9**) favour higher l/b ratios. For bite angles below 90° , however, Casey reported a deleterious effect of electron-withdrawing groups and thus the effect on **L7** and **L9** could be either way. In dissymmetric diphos ligands the electron withdrawing phosphine occupies the equatorial position and this leads to an increase of l/b .³⁹ The most regioselective ligand is ferrocene-type bisphosphine **L9** but the l/b ratio of 3.4 is smaller than those of the nonchiral derivatives in literature (l/b ratios from 5.4 to 11.4 for DPPF ligands).^{40,41} **L9**

is highly sterically hindered and the hampered π -stacking may also contribute to the modest, positive effect caused by the equatorial electron-withdrawing phosphine.



Scheme 2 Chiral ligand scope for rhodium-catalyzed hydroformylation.

Table 4 Hydroformylation of 1-octene with chiral bisphosphines.^a

Ligand	P–Rh–P (°) ^b	Conv. (%)	Aldehyde Sel. (%)	l/b ratio
L3	125	96	100	1.5
L4	121	99	100	1.9
L5	91	100	6	1.4
L6	105	99	100	2.2
L7	91	100	97	2.8
L8	95	100	5	0.8
L9	---	100	100	3.4

^a Reaction conditions: P(CO)/P(H₂) = 1, P(CO/H₂) = 20 bar, substrate/L/Rh = 1000/2/1,

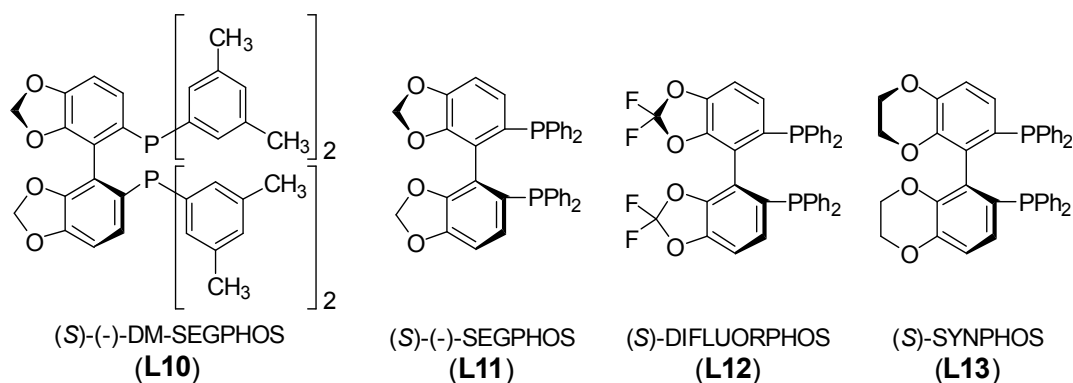
Rh(acac)(CO)₂ = 1 mM. 80 °C, 12 hrs. ^b Calculated P–Rh–P bond angles in

HRh(CO)₂(P–P) (**ee**); optimization of **L9** could not be achieved probably due to the steric bulkiness. Note that the bite angles reported here are those calculated for the trigonal-bipyramidal rhodium complexes and that they are not "natural bite angles" calculated with MM2 according to Casey and Whitteker, using a dummy atom without angular preferences⁴².

Asymmetric Hydroformylation of Styrene with Chiral Ligands

Screening of **L3–L13** as new bisphosphine ligands in hydroformylation of styrene revealed very high regioselectivities in all cases except for **L4** (Scheme 3, eq 4, Table 5). In all other instances the formation of the branched aldehyde was preferred and even exclusive formation of the branched product was seen for **L5** and **L8**; interestingly these are the ligands that gave mainly isomerization for 1-octene as the substrate, indicating that the terminal alkyl-Rh is not very stable. Comparison of **L7** and **L8** indicates that electron-donating groups on the phosphine aryl rings reduces the catalytic activity and enantioselectivity. A similar electronic effect is also demonstrated in the case of **L12** and **L11**, where fluorine substitution on the backbone has increased the conversion from 20% to 39%. The trend of inhibited activity by electron rich ligands cannot be generalized to a wider scope as the electron-richer methyl derivative **L10** has slightly higher conversion than its parent complex **L11** in Scheme 3. The formation of linear aldehyde is favored with less basic phosphine ligands as indicated by a trend of l/b of 0 (**L8**) < 0.09 (**L10**) < 0.56 (**L11**). We did observe a correlation of ligand basicity on the one hand and enantioselectivity and linear preference on the other hand within the SEGPHOS ligands **L8**, **L10** and **L11**. The increase of enantiomeric excess runs in parallel with a decrease of ligand basicity: 19% (**L8**) < 22% (**L10**) < 29% (**L11**), although the ee range is too small to arrive at a firm conclusion.

The highest enantioselectivity of 53% ee was obtained for (S)-BTFM-Garphos (**L7**) with the electron-withdrawing CF₃ substituents. **L7** seems to have the greatest potential in asymmetric hydroformylation evidenced as well by its high activity and a good branched preference.



Scheme 3 New Ligands for asymmetric hydroformylation of styrene.

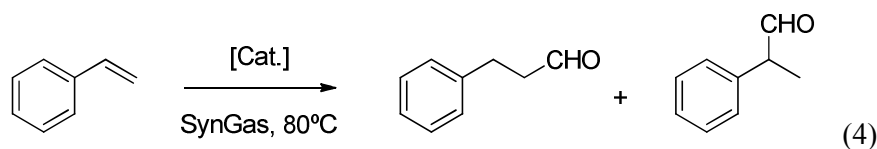


Table 5 Hydroformylation of styrene with chiral bisphosphines.^a

Ligand	Conv. (%)	Aldehyde Sel. (%)	l/b ratio	ee (S) (%)
L3	98	100	14/86	-3
L4	98	100	50/50	1
L5	11	100	--/100	-21
L6	100	100	7/93	-4
L7	100	100	7/93	53
L8	12	100	--/100	19

L9	100	96	13/83	-11
L9^b	65	100	10/90	-2
L10	23	100	8/92	22
L11	20	100	36/64	29
L12	39	100	9/91	33
L13	18	100	8/92	19

^a Reaction conditions: P(CO)/P(H₂) = 1, P(CO/H₂) = 20 bar, substrate/L/Rh = 1000/2/1, Rh(acac)(CO)₂ = 1 mM. , incubation 80 °C, 1 hr, reaction 80 °C, 12 hrs. ^b L/M = 10: excess ligand inhibits conversion and ee.

Condition Optimization of Hydroformylation with L7

With the promising results for **L7** in asymmetric hydroformylation under the “standard” condition, the reaction parameters such as T, P, solvent, incubation and L/M were varied to optimize the ee as shown in Table 6. Exclusive formation of aldehyde product was observed in all cases. The reaction time of 12 h is necessary to drive the reaction to completion (entry 1 vs 2). The process of catalyst pretreatment does not affect the enantioselectivity much (entry 1 vs 5). The optimal pressure is 20 bar as a poor enantioselectivity of 4% ee was obtained at 8 bar and the selectivity was not further increased using a higher pressure of 30 bar (entry 1 vs 3, 5 vs 6). Addition of excess ligand (L/M = 2) is critical to maintain the enantiomeric excess around 50% (entry 2 vs 9). Increasing the ligand/metal ratio to 5 equivalents slightly hampered the catalyst performance (entry 1 vs 10). The influence of ligand excess and pressure cannot be generally applied to all bisphosphine ligands as the opposite trend was seen for **L8** (see SI, Table S-1).

Table 6 Results of hydroformylation of styrene with **L7** under different conditions. ^a

#	Incubation ^b	Reaction	L/ M	Solvent	Conv. (%)	l/b ratio	ee (%)
1	80 °C	80	2	Toluene	100	7/93	53
2	80 °C	80 °C/20bar/8h	2	Tol	95	10/90	45
3	80 °C	80 °C/30b/12h	2	Tol	97	10/90	46
4	60 °C	60 °C/20b/12h	2	Tol	50	8/92	48
5	None	80 °C/20b/12h	2	Tol	98	10/90	48
6	None	80 °C/8b/12h	2	Tol	98	41/59	4
7	80 °C	80 °C/20b/12h	2	2-MeTHF	81	52/48	2
8	80 °C	80 °C/20b/12h	2	c-hexane	70	17/83	39
9	80 °C	80 °C/20b/8h	1.2	Tol	48	30/70	28
1	80 °C	80 °C/20b/12h	5	Tol	99	10/90	49

^a Exclusive formation of aldehyde was observed in all entries. ^b Incubation condition: 10 bar of CO/H₂ (1:1) for 1 h.

To understand the better catalytic performance of **L7**, *in situ* HPIR experiments for **L7** were performed under the catalytic conditions (80 °C, 20 bar). At the beginning of heating, the catalyst precursor **1** was observed with two absorptions at 2082 and 2011 cm⁻¹ in the terminal carbonyl region (Fig. 5). When the temperature increased to 65 °C, **1** was completely converted to a new species, assigned to HRh(CO)₂(**L7**) with a pair of absorptions at 2010 and 1970 cm⁻¹. The carbonyl bands of HRh(CO)₂(**L7**) shift to higher wavenumbers (respectively 18 and 27 cm⁻¹) compared to HRh(CO)₂(**L1**), consistent with the electron deficiency in **L7**. Additional evidence for the **ea** structure of HRh(CO)₂(**L7**) was seen from the HP-NMR spectra (Fig. 6). Similar to **ea**-HRh(CO)₂(**L1**) (Table 2, δ -8.78, $^1J_{\text{Rh-H}} = 10.8$ Hz, $^2J_{\text{P-H}} = 44.7$ Hz), the ¹H NMR of HRh(CO)₂(**L7**) showed a typical triplet of doublets at δ -9.21 with $^1J_{\text{Rh-H}} = 9.6$ Hz and $^2J_{\text{P-H}} = 62.5$ Hz for the hydride resonances. Consistently, a doublet signal at δ 44.71 ($^1J_{\text{Rh-P}} = 120.0$ Hz) was observed in ³¹P{¹H} NMR (**ea**-HRh(CO)₂(**L1**): δ 28.03, $^1J_{\text{Rh-P}} = 117.4$ Hz) and the H-P coupling constant of 63.5 Hz was obtained from ³¹P NMR (see SI, Fig. S-3 and S-4). The smaller $^1J_{\text{Rh-H}}$ and larger $^1J_{\text{Rh-P}}$ are indicative of the non-

basicity of L7 relative to L1 and BDPP.

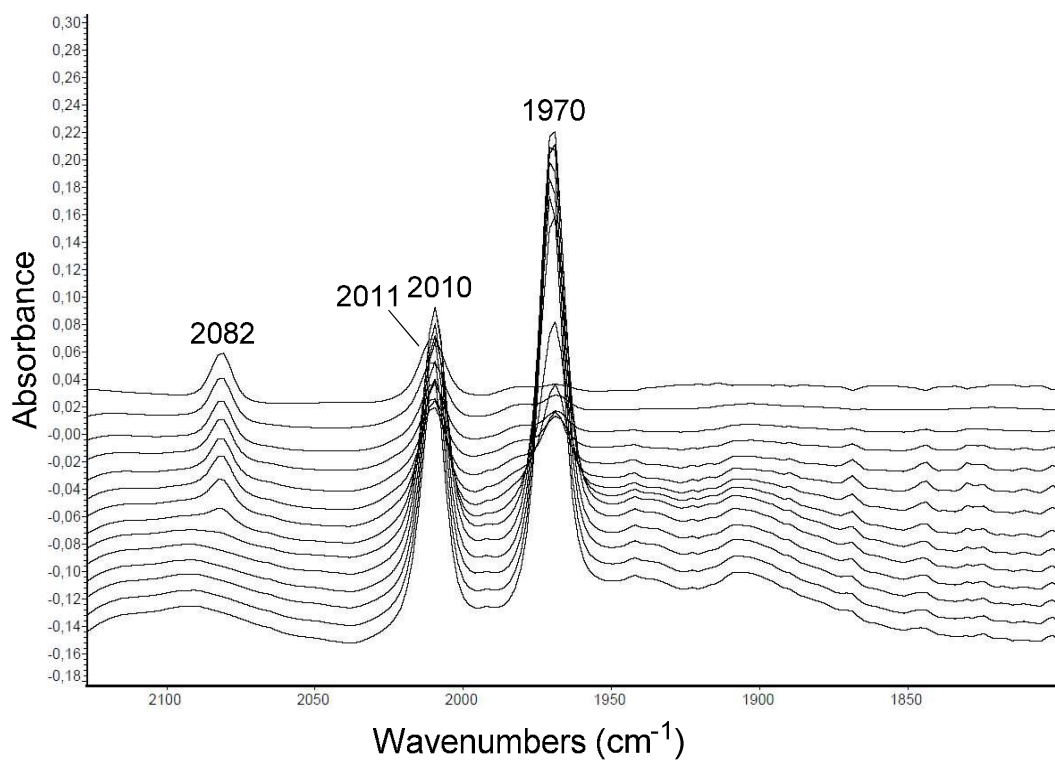


Fig. 5 HP-FTIR spectra for the reaction of **1** with L7 in 2-MeTHF at 80 °C, 20 bar of CO/H₂ (1:1) (carbonyl region). Spectra were recorded from top to bottom.

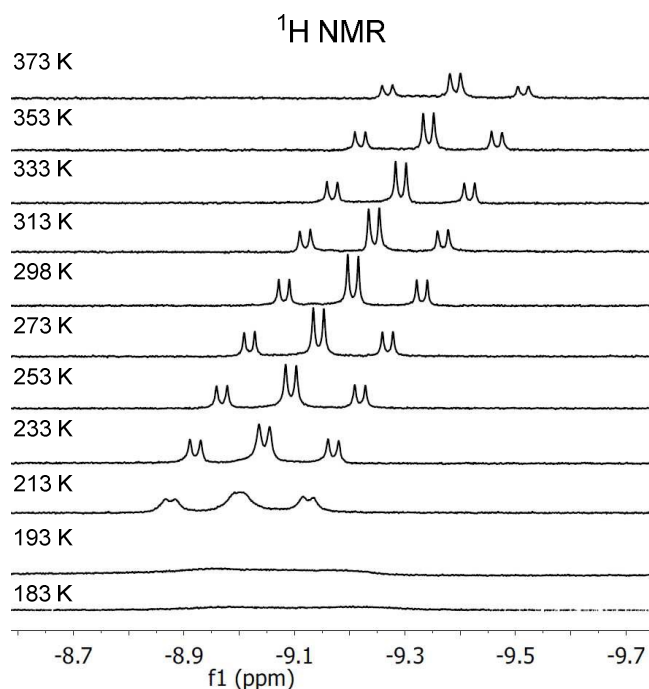


Fig. 6 ^1H NMR spectra (hydride region) for the reaction of **1** with **L7** in Toluene- d_8 at 80 °C, 10 bar of CO/H_2 (1:1) after 1 h.

L6 has a calculated bite angle of 105° , slightly wider than that of **L7**. The IR spectra recorded under catalytic conditions showed the formation of a mixture of intermediates. The dominating resting state is $\text{HRh}(\text{CO})_2(\text{L6})$ with the two absorptions at 1990 and 1948 cm^{-1} (Fig. 7(a)). There are other weak bands appearing at 2046, 2014, 2004, 1797 cm^{-1} which can probably be attributed to rhodium carbonyl species or/and the equatorial-equatorial isomer of $\text{HRh}(\text{CO})_2(\text{L6})$. Under the same experimental conditions, the IR spectra of **L4** revealed two absorptions of terminal carbonyl stretching at 2044, 1967 cm^{-1} from the beginning of heating (Fig. 7(b)). This suggests a rapid formation of the resting state $\text{HRh}(\text{CO})_2(\text{L4})$. The higher frequencies of the carbonyl stretching vibrations of $\text{HRh}(\text{CO})_2(\text{L4})$ are in accordance with the equatorial-equatorial coordination of the bisphosphine, which can be expected from its calculated natural bite angle of around 120° . The exceptional *ee* geometry of $\text{HRh}(\text{CO})_2(\text{L4})$ can

explain the formation of linear aldehyde for styrene ($l/b = 1/1$) as shown in Table 5, similar to Xantphos ($l/b = 4.7/5.3$).¹²

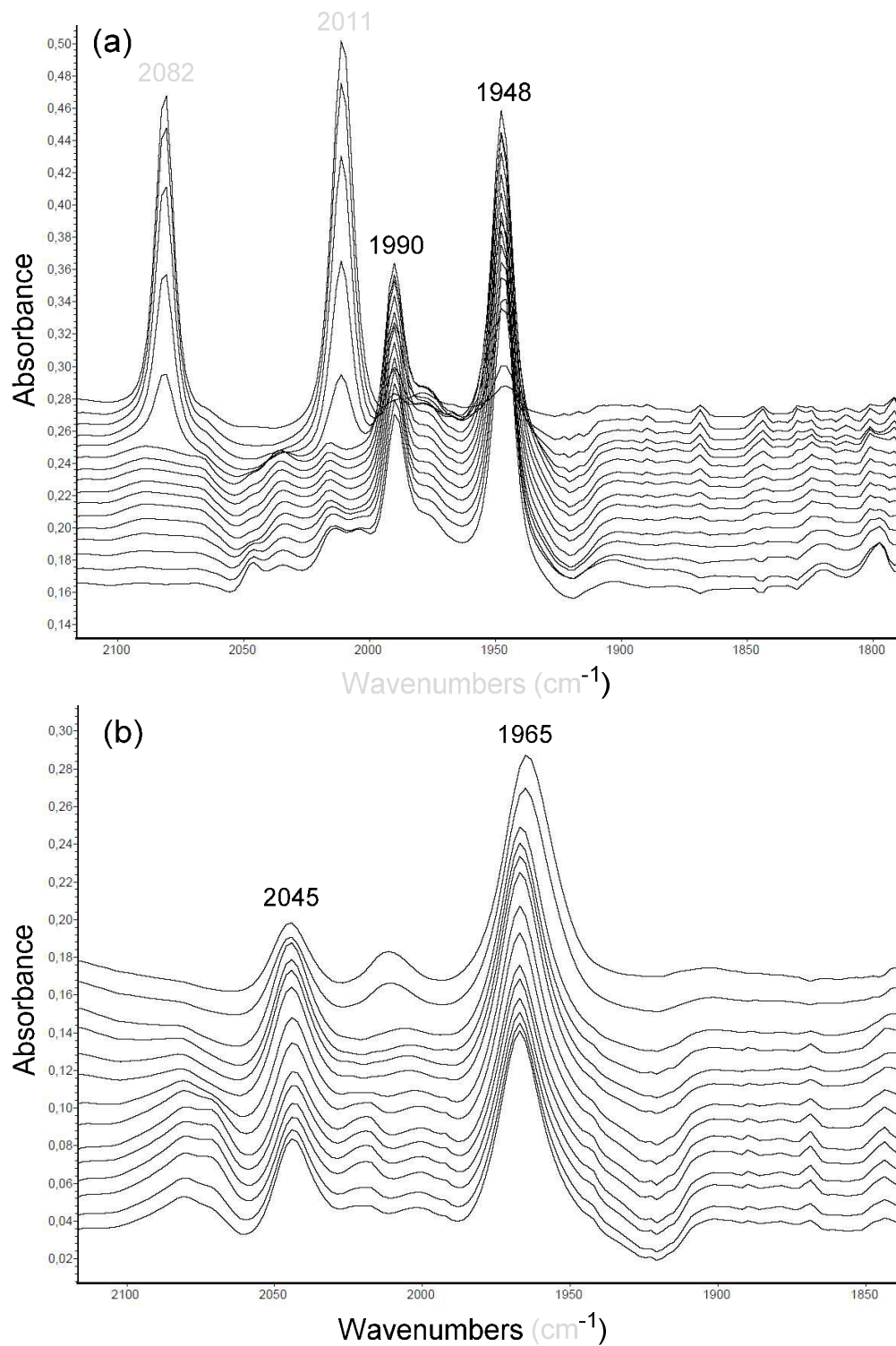


Fig. 7 (a) HP-FTIR spectra for the reaction of **1** with **L6** in 2-MeTHF at 80 °C, 20 bar of CO/H₂ (1:1) (carbonyl region). (b) HP-FTIR spectra for the reaction of **1** with **L4** in 2-MeTHF at 80 °C, 20 bar of CO/H₂ (1:1) (carbonyl region). Spectra were recorded from top to bottom.

Calculated free energy differences between isomers.

We have calculated the free energies of the two coordination modes (**ea** and **ee**) of HRh(CO)₂(P–P) in both gas phase and solution, using the Polarizable Continuum Model (PCM), see Table 7. Calculations with the B3LYP hybrid functional including PCM seem generally in better agreement with the IR observations than those with the M062 functional. Nonetheless, the energy difference between isomers seems overestimated for **L7** by B3LYP/PCM. Dominating **ea** geometry is seen in cases of **L7**, BDPP and CHIRAPHOS, where the free energy differences between **ee** and **ea** isomers are over 2 kcal·mol⁻¹, equivalent to a ratio of **ea/ee** of ~ 30. Isomers with smaller free energy differences display little preferences in geometry distributions for ligands such as SPANphos, DPEphos, pySPAN and monodentate phosphines. As one can see from the table we have obtained excellent agreement between calculated energies and experimentally observed isomer distributions.

Table 7 Free energies (kcal·mol⁻¹) for stationary points in the two coordination modes (**ea** and **ee**) of HRh(CO)₂(bisphosphine) in comparison with experimentally observed coordination modes. Toluene was used as the solvent in PCM.

Ligand	Isomer (observed)	$\Delta G_{ea} - \Delta G_{ee}$ (kcal·mol ⁻¹) of HRh(CO) ₂ (bisphosphine)			
		B3LYP/LANL2DZ		M062/LANL2DZ	
		Gas Phase	PCM	Gas Phase	PCM

L7	ea	-2.51	-3.52	-1.22	-1.52
BDPP	ea	-2.45	-2.76	-2.21	-2.58
L6	ea	-1.6	-2.74	-1.35	-2.14
CHIRAPHOS	ea	-2.18	-2.18	-1.55	-1.58
SPANphos	ee/ea	-0.64	-1.3	-2.3	-2.44
L1	ea	-0.57	-1.09	-0.24	-0.81
2 PPh ₃	ee/ea ^a	0.94	0.16	-2.8	-2.37
2 PEtPh ₂	ee/ea	1.22	0.24	0.24	-0.51
L4	ee	0.73	0.65	-1.19	0.19
pySPAN	ee	1.63	1.68	-1.35	-1.37
L2	none	2.14	2.31	3.29	2.84

^a The major isomer has **ee** coordination mode.

Solvent effects were also studied under the “standard” conditions. As previously mentioned, *in situ* HP-IR studies of the catalyst pretreatment using **L7** in 2-MeTHF displayed the successful formation of **ea**-HRh(CO)₂(**L7**). However, the actual hydroformylation reaction of styrene in 2-MeTHF is much less regioselective and enantioselective than that in toluene (Table 6, entry 1 vs 7). Cyclohexane, less polar than toluene, also gave a slower reaction. Attempts to clarify the origin of solvent effect in **L7** were undertaken by DFT calculations. Both the **ea/ee** ratio and the interaction energy difference go up, opposite to the decline of the interaction energy between rhodium and the ligand, as the solvent polarity increases (Table 8). It remains unclear how the solvent affects the rate of reaction in the current work. Perhaps the solvent can play a directing role in the geometry of alkene coordination by competitive interaction with the metal center; this is beyond the scope of the present paper.

Table 8 Free energies ($\text{kcal}\cdot\text{mol}^{-1}$) for stationary points in the two coordination modes (**ea** and **ee**) of $\text{HRh}(\text{CO})_2(\text{L7})$ using PCM for three solvents: *n*-hexane, toluene and tetrahydrofuran.

Solvent	$\Delta G_{\text{ea}} - \Delta G_{\text{ee}} (\text{kcal}\cdot\text{mol}^{-1})$		$E_{\text{interaction}} (\text{kcal}\cdot\text{mol}^{-1})^{\text{a}}$			
	B3LYP/LANL2DZ	M062/LANL2DZ	B3LYP/LANL2DZ		M062/LANL2DZ	
			ea	ee	ea	ee
Gas phase	-2.51	-1.22	-30.68	-28.18	-38.79	-37.57
<i>n</i> -Hexane	-3.30	-1.45	-29.57	-26.27	-36.93	-35.48
Toluene	-3.52	-1.52	-29.20	-25.68	-36.52	-35.00
THF	-4.15	-1.76	-26.98	-22.84	-34.58	-32.82

^a $E_{\text{interaction}}$ is the interaction energy between **L7** and the metal center. It is calculated with the equation $E_{\text{interaction}} = E(\text{HRh}(\text{CO})_2(\text{L7})) - E([\text{HRh}(\text{CO})_2]) - E(\text{L7})$.

Conclusions

A series of new bisphosphine ligands has been examined in rhodium-catalyzed hydroformylation. The presence of (bisphosphine) $\text{Rh}(\text{CO})_2\text{H}$ was detected by HP-IR and HP-NMR spectra in selected cases. The low selectivity in 1-octene hydroformylation for DTP-DPEphos (**L2**) can be explained by the difficulty of the bulky ligand to coordinate to the rhodium center in its competition with CO, while its parent bisphosphine DPEphos (**L1**) forms stable, active catalysts under the conditions. Both spectroscopic and theoretical studies indicate that the **ee/ea** equilibrium is controlled by the steric factor of the bisphosphines. Exclusive formation of **ea** isomers was seen for the ligands with small bite angles of around 100° . For CTH-(R)-BINAM (**L4**), which has a wider bite angle of around 120° , both phosphorus atoms chelate in the

equatorial sites. Moreover, a simple correlation between **ea/ee** ratio and the **l/b** ratio does not exist within the scope of this work. **L4**, obtained by replacing the methylene groups in NAPHOS by NH, displays structural similarity with the well performing NAPHOS-type ligand (**l/b** = 99) and adopts an equatorial-equatorial resting state in HRh(CO)₂(**L4**). However, the **l/b** ratio is low in the hydroformylation of 1-octene with **L4**. The poor regioselectivity of **L4** disproved once again that a wide bite angle cannot be used as the exclusive parameter in predicting the linear selectivity in hydroformylation reactions. Instead, the electronic change brought about by heteroatom incorporation dramatically lowers the selectivity. For 1-octene hydroformylation, the highest linearity was achieved with the less basic bisphosphine **L7** and the ferrocene bisphosphine **L9**. Hence, within the ligands for rhodium-catalyzed hydroformylation considered in this paper, it appears that electronic control is more important than bite angle. Among all the bisphosphine complexes, **L7** was the most promising ligand for asymmetric hydroformylation of styrene with a high conversion and branched selectivity (**b/l** = 13) (53% ee), although better alternatives are available from literature. We have shown that DFT can very well predict the structure of the resting state HRh(CO)₂(P–P), be it equatorial-equatorial or equatorial-apical, which offers a useful alternative in case *in situ* NMR or IR would not be available.

Acknowledgements

Y.J. thanks the Institute of Chemical Research of Catalonia (ICIQ), 43007 Tarragona, Spain for hosting her, and Syngaschem BV for enabling her stay in The Netherlands and Spain. Syngaschem BV acknowledges financial support from Synfuels China Technology Co. Ltd.

Supporting Information Available: $^{31}\text{P}\{^1\text{H}\}$ and ^{31}P NMR spectra, results of hydroformylation of styrene with **L8**, incubation test, a complete citation of gaussian and a summary of coordinates and energies for calculated complexes.

References

- 1 C. Claver and P. W. N. M. van Leeuwen, *Rhodium Catalyzed Hydroformylation*, Kluwer Academic Publishers: Dordrecht, 2000.
- 2 A. Behr and P. Neubert, *Applied Homogeneous Catalysis*, John Wiley & Sons, Weinheim, 2012.
- 3 B. Cornils and W. A. Herrmann, *Applied Homogeneous Catalysis with Organometallic Compounds: A Comprehensive Handbook in Three Volumes, Volume 3*, Wiley, Weinheim, 2002.
- 4 J. Klosin and C. R. Landis, *Acc. Chem. Res.*, 2007, **40**, 1251.
- 5 R. Franke, D. Selent and A. Börner, *Chem. Rev.*, 2012, **112**, 5675.
- 6 R. I. McDonald, G. W. Wong, R. P. Neupane, S. S. Stahl and C. R. Landis, *J. Am. Chem. Soc.*, 2010, **132**, 14027.
- 7 S. Gladiali, J. C. Bayon and C. Claver, *Tetrahedron: Asymmetry*, 1995, **6**, 1453.
- 8 F. Agbossou, J. F. Carpentier and A. Mortreux, *Chem. Rev.*, 1995, **95**, 2485.
- 9 Y. Pottier, A. Mortreux and F. Petit, *J. Organomet. Chem.*, 1989, **370**, 333.
- 10 N. Sakai, S. Mano, K. Nozaki and H. Takaya, *J. Am. Chem. Soc.*, 1993, **115**, 7033.
- 11 G. J. H. Buisman, M. E. Martin, E. J. Vos, A. Klootwijk, P. C. J. Kamer and P. W. N. M. van Leeuwen, *TetrahedronAsymmetry*, 1995, **6**, 719.
- 12 M. Kranenburg, Y. E. M. van der Burgt, P. C. J. Kamer, P. W. N. M. van

- Leeuwen, K. Goubitz and J. Fraanje, *Organometallics*, 1995, **14**, 3081.
- 13 L. A. van der Veen, P. C. J. Kamer and P. W. N. M. van Leeuwen, *Organometallics*, 1999, **18**, 4765.
- 14 L. A. van der Veen, M. D. K. Boele, F. R. Bregman, P. C. J. Kamer, P. W. N. M. van Leeuwen, K. Goubitz, J. Fraanje, H. Schenk and C. Bo, *J. Am. Chem. Soc.*, 1998, **120**, 11616.
- 15 L. A. van der Veen, P. C. J. Kamer and P. W. N. M. van Leeuwen, *Angew. Chem. Int. Ed.*, 1999, **38**, 336.
- 16 H. Klein, R. Jackstell, K.-D. Wiese, C. Borgmann and M. Beller, *Angew. Chem. Int. Ed.*, 2001, **40**, 3408.
- 17 O. Diebolt, H. Tricas, Z. Freixa and P. W. N. M. van Leeuwen, *ACS Catal.*, 2013, **3**, 128.
- 18 E. Boymans, M. Janssen, C. Müller, M. Lutz and D. Vogt, *Dalt. Trans.*, 2013, **42**, 137.
- 19 F. A. Rampf, M. Spiegler and W. A. Herrmann, *J. Organomet. Chem.*, 1999, **582**, 204.
- 20 L. A. Van Der Veen, P. H. Keeven, G. C. Schoemaker, J. N. H. Reek, P. C. J. Kamer, P. W. N. M. Van Leeuwen, M. Lutz and A. L. Spek, *Organometallics*, 2000, **19**, 872.
- 21 A. R. Sanger, *J. Mol. Catal.*, 1978, **3**, 221.
- 22 A. R. Sanger and L. R. Schallig, *J. Mol. Catal.*, 1977, **3**, 101.
- 23 R. W. Eckl, T. Priermeier and W. A. Herrmann, *J. Organomet. Chem.*, 1997, **532**, 243.
- 24 C. P. Casey, E. L. Paulsen, E. W. Beuttenmueller, B. R. Proft, L. M. Petrovich, B. A. Matter and D. R. Powell, *J. Am. Chem. Soc.*, 1997, **119**, 11817.

- 25 P. C. J. Kamer, A. van Rooy, G. C. Schoemaker and P. W. N. M. van Leeuwen, *Coord. Chem. Rev.*, 2004, **248**, 2409.
- 26 C. Xia, Y. Sun and D. Li, *Fenzi Cuihua*, 1989, **3**, 62.
- 27 R. M. Deshpande, S. S. Divekar, B. M. Bhanage and R. V. Chaudhari, *J. Mol. Cat.*, 1992, **77**, 13.
- 28 A. D. Becke, *J. Chem. Phys.*, 1993, **98**, 5648.
- 29 Y. Zhao and D. G. Truhlar, *Theor. Chem. Acc.*, 2008, **120**, 215.
- 30 M. J. Frisch, *et al.*, *Gaussian, Inc., Wallingford CT*, 2013.
- 31 K. H. Shaughnessy, P. Kim and J. F. Hartwig, *J. Am. Chem. Soc.*, 1999, **121**, 2123.
- 32 B. C. Hamann and J. F. Hartwig, *J. Am. Chem. Soc.*, 1998, **120**, 3694.
- 33 J. J. Carbó, F. Maseras, C. Bo and P. W. N. M. van Leeuwen, *J. Am. Chem. Soc.*, 2001, **123**, 7630.
- 34 I. del Río, W. G. J. de Lange, P. W. N. M. van Leeuwen and C. Claver, *J. Chem. Soc. Dalt. Trans.*, 2001, **2**, 1293.
- 35 C. Li, L. Guo and M. Garland, *Organometallics*, 2004, **23**, 2201.
- 36 A. Castellanos-Paez, S. Castillon, C. Claver, P. W. N. M. van Leeuwen and W. G. J. de Lange, *Organometallics*, 1998, **17**, 2543.
- 37 E. Rafter, D. G. Gilheany, J. N. H. Reek and P. W. N. M. van Leeuwen, *ChemCatChem*, 2010, **2**, 387.
- 38 E. J. Zipp, I. Van Der Vlugt, D. M. Tooke, L. Spek and D. Vogt, *Dalt. Trans.*, 2005, 512.
- 39 C. P. Casey, E. L. Paulsen, E. W. Beuttenmueller, B. R. Proft, B. A. Matter and D. R. Powell, *J. Am. Chem. Soc.*, 1999, **121**, 63.
- 40 J. D. Unruh and W. J. Wells, *Belgian Pat. 840, 906*, 1976.

- 41 J. D. Unruh and J. R. Christenson, *J. Mol. Catal.*, 1982, **14**, 19.
- 42 C. P. Casey and G. T. Whiteker, *Isr. J. Chem.*, 1990, **30**, 299.

TOC for

**Ligand Effects in Rhodium-Catalyzed Hydroformylation with
Bisphosphines: Steric or Electronic?**

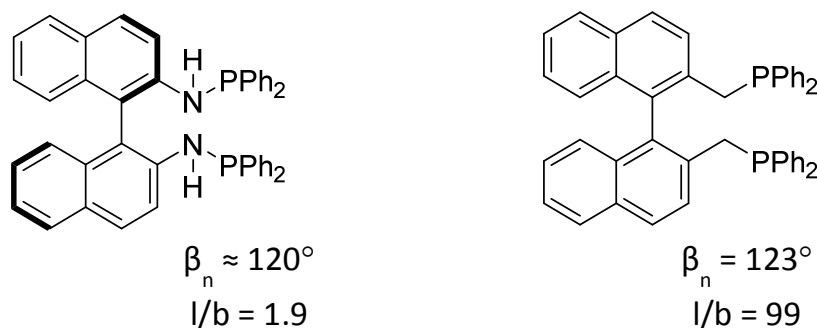
Yunzhe Jiao^{*†‡}, Marta Serrano Torne[‡], Jose Gracia[†], J. W. (Hans) Niemantsverdriet^{†#}
and Piet W. N. M. van Leeuwen^{*‡&}

[‡]*Institute of Chemical Research of Catalonia (ICIQ), The Barcelona Institute of Science
and Technology, Avda. Països Catalans 16, 43007 Tarragona, Spain*

[†]*SynCat@Beijing, Synfuels China Technology Co. Ltd, Beijing, P. R. China*

[#]*Syngaschem BV, PO Box 6336, 5600 HH Eindhoven, The Netherlands*

[&]*Present address: LPCNO, INSA-Toulouse, 135 Avenue de Rangueil, F-31077 Toulouse, France*



Do wide bite angles lead to high linear regioselectivity in
hydroformylation, or is an electronic effect operative?